Journal of Virology, Mar. 2009, p. 2575–2583 0022-538X/09/\$08.00+0 doi:10.1128/JVI.02133-08 Copyright © 2009, American Society for Microbiology. All Rights Reserved.

Determinants Flanking the CD4 Binding Loop Modulate Macrophage Tropism of Human Immunodeficiency Virus Type 1 R5 Envelopes [∇]†

Maria José Duenas-Decamp, Paul J. Peters, Dennis Burton, and Paul R. Clapham*

Program in Molecular Medicine and Department of Molecular Genetics and Microbiology, University of Massachusetts Medical School, Worcester, Massachusetts 01605, and the Scripps Research Institute, Department of Immunology, IMM2, La Jolla, California 92037²

Received 9 October 2008/Accepted 29 December 2008

Human immunodeficiency virus type 1 R5 viruses vary extensively in phenotype. Thus, R5 envelopes (env) in the brain tissue of individuals with neurological complications are frequently highly macrophage-tropic. Macrophage tropism correlates with the capacity of the envelope to exploit low CD4 levels for infection. In addition, the presence of an asparagine at residue 283 within the CD4 binding site has been associated with brain-derived envelopes, increased env-CD4 affinity, and enhanced macrophage tropism. Here, we identify additional envelope determinants of R5 macrophage tropism. We compared highly macrophage-tropic (B33) and non-macrophage-tropic (LN40) envelopes from brain and lymph node specimens of one individual. We first examined the role of residue 283 in macrophage tropism. Introduction of N283 into LN40 (T283N) conferred efficient macrophage infectivity. In contrast, substitution of N283 for the more conserved threonine in B33 had little effect on macrophage infection. Thus, B33 carried determinants for macrophage tropism that were independent of N283. We prepared chimeric B33/LN40 envelopes and used site-directed mutagenesis to identify additional determinants. The determinants of macrophage tropism that were identified included residues on the CD4 binding loop flanks that were proximal to CD4 contact residues and residues in the V3 loop. The same residues affected sensitivity to CD4-immunoglobulin G inhibition, consistent with an altered env-CD4 affinity. We predict that these determinants alter exposure of CD4 contact residues. Moreover, the CD4 binding loop flanks are variable and may contribute to a general mechanism for protecting proximal CD4 contact residues from neutralizing antibodies. Our results have relevance for env-based vaccines that will need to expose critical CD4 contact residues to the immune system.

Human immunodeficiency virus type 1 (HIV-1) requires interactions between viral envelope glycoproteins and cell surface CD4 and coreceptors to trigger fusion and entry into cells. HIV-1 R5 viruses that specifically use CCR5 as a coreceptor are those predominantly transmitted (3). Yet, our knowledge of R5 virus variation in different biological properties is still limited. In vivo, HIV-1 infection is limited mostly to cells that express CD4 and appropriate coreceptors. Thus, HIV-1 infects CD4⁺ T cells, monocyte/macrophage lineage cells, and dendritic cells. CCR5 is expressed on each of these cell lineages, although on T cells, CCR5 is restricted mainly to RO45⁺ memory cells (1, 16). Early in infection, R5 viruses target and decimate mucosal CD4⁺ memory T cells (2, 18, 26). R5 viruses are also predominant in tissues in which monocyte/macrophage lineage cells are prevalent, and several reports have described the presence of highly macrophage-tropic R5 viruses in brain tissue (11, 12, 20, 22). Previously, we used PCR to amplify HIV-1 envelope genes directly from patient tissues. We found that R5 virus envelopes amplified from brain tissue frequently conferred highly efficient infection of macrophages, while the majority of those from lymph nodes, blood, and semen infected macrophages inefficiently (20, 22). Although

those studies examined relatively few infected individuals, they demonstrated over 1,000-fold variation in macrophage-tropic HIV-1 R5 viruses. Such variation is likely to have a significant impact on transmission and pathogenesis.

The envelope (env) determinants of R5 macrophage-tropic strains are poorly understood. Several studies have shown that highly macrophage-tropic brain envelopes are able to exploit low levels of CD4 on macrophages for infection, consistent with an enhanced interaction between gp120 and CD4. Dunfee et al. reported that an asparagine residue at position 283 in the C2 part of the CD4 binding site was present in 41% of envelope sequences from brain tissue specimens of patients with HIV-associated dementia and in only 8% of envelopes from non-HIV-associated dementia brain tissue (8). The same study showed that the presence of N283 (rather than the more conserved T283) led to an increased affinity of gp120 for CD4, probably because the side chain of asparagine could more readily form a hydrogen bond with Q40 on CD4. However, our previous data showed that N283 is not the only determinant of macrophage infectivity, since several macrophage-tropic R5 envelopes from brain and semen specimens lacked N283, while non-macrophage-tropic envelopes from lymph node specimens carrying N283 were identified (22). Dunfee et al. also reported that a glycosylation site at residue 386, close to the CD4 binding loop, influenced exposure of the CD4 binding site and had an impact on macrophage tropism and sensitivity to the CD4 binding site antibody b12 (9). We have recently confirmed a role for N386 in resistance to the CD4 binding site monoclonal antibody (MAb) b12. However, resistance was dependent on

^{*} Corresponding author. Mailing address: Program in Molecular Medicine, University of Massachusetts Medical School, Biotech II Suite 315, 373 Plantation St., Worcester, MA 01605. Phone: (508) 856-6281. Fax: (508) 856-4283. E-mail: paul.clapham@umassmed.edu.

[†] Supplemental material for this article may be found at http://jvi.asm.org/.

[▽] Published ahead of print on 7 January 2009.

the presence of a proximal residue, R373, which acted together with N386 to block b12 (7).

Here, we have further investigated envelope determinants of macrophage tropism by preparing chimeric envelopes from highly macrophage-tropic and non-macrophage-tropic R5 envelopes from brain and lymph node specimens from the same subject. We show that R5 macrophage tropism is controlled by several determinants in gp120 that are focused on amino acids flanking the CD4 binding loop, with a contribution from residues in the V3 loop.

MATERIALS AND METHODS

Envelopes and molecular constructs for cotransfection and pseudovirion production. HIV-1 envelopes described here were derived from subject NA420, a heterosexual patient with no cognitive impairment and sparse-infiltrate giant-cell encephalitis who died of AIDS. Samples from lymph node (LN) and frontal lobe brain tissue were obtained at autopsy and kept frozen at -80°C . DNA was extracted as described previously (24). PCR amplification of complete envelopes was performed as described previously (20). Patient NA420's envelope genes were cloned into pSVIIIenv by using conserved KpnI sites (10) and into pBluescript for direct mutagenesis.

Cells. 293T cells (6) were used to prepare env-containing (env⁺) pseudovirions by transfection. HeLa TZM-bl cells were used to titrate env+ pseudovirions and to evaluate HIV-1 neutralization. HeLa TZM-bl cells express high levels of CD4 and CCR5 and contain β-galactosidase and luciferase reporter genes under the control of an HIV long terminal repeat (23, 27). The RC49 cell line is a clone of the HeLa/CD4/CCR5 cells that express low levels of CD4 (23). Macrophage cultures were prepared from elutriated monocytes (14), which were provided by the University of Massachusetts Center for AIDS Research Elutriation Core. The elutriated monocytes were cultured for 2 days in medium containing macrophage colony-stimulating factor (R&D Systems) and for an additional 5 days in medium lacking macrophage colony-stimulating factor and then used for virus infections. Alternatively, macrophages were prepared from blood monocytes by adherence as described previously (20). On the day prior to infection, the macrophages were washed three times in Versene and incubated at 37°C for 10 min to loosen cell attachments. Macrophages were then gently scraped off and resuspended in RPMI 1640 medium containing 10% human serum, counted, and seeded into 48-well tissue culture travs at 1.25×10^5 cells per well.

Direct mutagenesis. Site-directed mutagenesis was carried out using a QuikChange site-directed mutagenesis kit (Stratagene Inc.) using gp160 in pBluescript plasmids as templates and mutagenic primers to introduce mutations. The presence of the desired mutations was confirmed by sequencing the insert. gp160 inserts containing the desired mutations were cloned into the pSVIIIenv vector via KpnI sites.

Production and titration of env⁺ **pseudovirions.** The env⁻ pNL4.3 construct and the pSVIIIenv expression vector were used to produce env⁺ pseudovirions as described previously (20, 22). Briefly, env⁺ pSVIIIenv with env⁻ pNL4.3 was cotransfected into 293T cells by using calcium phosphate. Cell supernatants carrying pseudovirions were harvested 48 h after transfection, clarified (1,000 \times g for 10 min), aliquoted, and stored at -152° C.

Comparison of env⁺ pseudotype virus infectivity of primary macrophages and RC49 cells with infectivity of HeLa TZM-bl cells. Pseudovirions carrying mutant and patient-derived envelopes were titrated with TZM-bl cells, RC49 cells that express low amounts of CD4 (23), and primary macrophages. TZM-bl and RC49 cells (2 × 10⁴ cells/well/0.5 ml) were seeded into 48-well trays on the day prior to infection, while macrophages were seeded at 1.25 × 10⁵ cells/well. A 0.1-ml volume of serially diluted (10-fold dilutions) cell-free virus supernatant was incubated with cells. Infections were performed in duplicate. After 3 h at 37°C, 0.4 ml of growth medium was added. For infection of HeLa TZM-bl, cells were fixed 2 days postinfection in phosphate-buffered saline (PBS)-0.5% glutaraldehyde at 4°C for 15 min. Cells were then washed twice with PBS-0.1% azide and once in PBS before being stained with X-Gal (0.5 mg of 5-bromo-4-chloro-3-indolyl-B-D-galactopyranoside/ml [Fisher Bioreagents Inc.], 3 mM potassium ferrocyanide, 3 mM potassium ferricyanide, 1 mM magnesium chloride) for 3 h.

For macrophages and HeLa RC49 cells (which do not have a β -galactosidase reporter gene), cells were fixed at 7 and 3 days postinfection, respectively, in a cold (-20° C) 1:1 mixture of methanol-acetone for 10 min at room temperature. Cells were then washed once with PBS-0.1% azide-1% fetal bovine serum, and a 1:1 mixture of anti-p24 MAbs, 38:96K and EF7 (Centre for AIDS Reagents, United Kingdom), was added. After 1 h at room temperature, the cells were

rinsed twice in PBS-0.1% azide-1% fetal bovine serum, and goat anti-mouse β -galactosidase conjugate was added at room temperature for 60 min. Cells were then washed twice with PBS-0.1% azide and once with PBS before being stained with X-Gal, as described above for HeLa TZM-bl cells. Since env⁺ pseudovirions are capable of only a single round of replication, we were able to estimate the number of focus-forming units (FFU) by counting individual or small groups of blue-stained, infected cells. Numbers of FFUs/ml were then calculated. For primary macrophages, cells were pretreated with 0.1 ml DEAE dextran (8 μ g/ml) in growth medium before virus supernatants were added. Infection of macrophages was also aided by spinoculation at 1,200 × g for 40 min (19).

The infectivity values for RC49 cells and macrophages were also estimated as a ratio of the infectivity of these cells to the infectivity of TZM-bl cells, and ratios are presented as a percentage of the ratio observed for B33 env $^+$ pseudovirions by using the following formula: (RC49 or macrophage titer/TZM-bl titer for mutant env $^+$ pseudovirions)/(RC49 or macrophage titer/TZM-bl titer for B33 $^+$ pseudovirions) \times 100. Error bars in figures were calculated from replicate wells for individual experiments.

PRO 542 inhibition assays. HeLa TZM-bl cells (0.1 ml) were seeded into 96-well trays at 8×10^4 cells/ml on the day prior to infection. Two hundred FFU of env+ pseudovirions was mixed with twofold serial dilutions of PRO 542 in a 50-µl volume. After 1 h of incubation at 37°C, these mixtures were added to target cells and incubated for an additional 3 h at 37°C. Then, the virus-antibody mixture was removed, growth medium was added, and infected cells were incubated at 37°C for 48 h. Medium was then removed, and 100 µl of medium without phenol red was added. Cells were then fixed and solubilized by adding 100 µl of Beta-Glo (Promega Inc.). Luminescence was then read with a BioTek Clarity luminometer.

 IC_{50} s and correlations. Virus 50% inhibitory concentrations (IC_{50} s) and correlations were calculated using Prism version 4.0c software for Macintosh. IC_{50} s were calculated by using a nonlinear regression analysis. In cases where inhibition did not completely eliminate infectivity, IC_{50} s were estimated manually from an Excel plot. Correlations were calculated by using a two-tailed, nonparametric Spearman test with 95% confidence limits.

RESULTS

Here, we have investigated envelope residues that determine macrophage infectivity for a highly macrophage-tropic HIV-1 envelope (B33) derived from brain tissue by comparison with a non-macrophage-tropic envelope (LN40) from lymph node tissue from the same individual (patient NA420). In the first part of the study, we identified envelope determinants that confer infection via low levels of cell surface CD4, using HeLa RC49 cells as a surrogate for infection of macrophages. We then confirmed that the residues identified modulated infectivity of primary macrophages.

The role of N283 in the capacity to exploit low cell surface **CD4 levels for infection.** Residue 283 in the C2 part of the CD4 binding site was previously shown to have a strong influence on the macrophage tropism of R5 envelopes (8). The presence of the asparagine residue at 283 (instead of the more conserved threonine) conferred an increase in macrophage infectivity and the capacity to infect cells via low levels of CD4. N283 also confers higher affinity for monomeric gp120 binding to soluble CD4 (sCD4), strongly suggesting that the capacity to exploit low CD4 levels results directly from an increased env-CD4 affinity (8). Threonine and isoleucine are the most common amino acids at residue 283 for subtype B viruses. Patient NA420's B33 envelope carries N283, while LN40 carries T283. We first made the following substitutions at residue 283, N283T and N283I in B33 (B33T and B33I, respectively) and T283N and T283I in LN40 (LN40N and LN40I, respectively), and tested the mutants' capacity to confer infection of HeLa cells via high and low levels of CD4. All the mutant envelopes conferred efficient infection of HeLa TZM-bl cells that express high levels of CD4 (Fig. 1A). LN40N conferred infectivity for

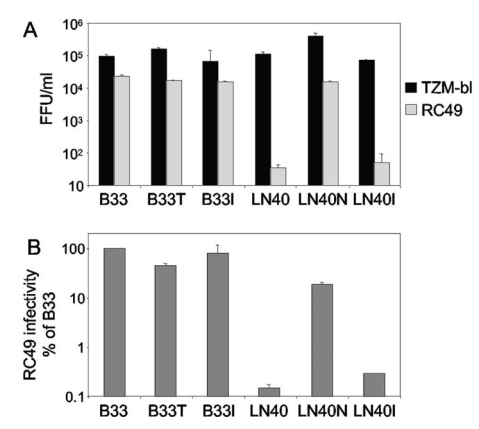


FIG. 1. Role of N283 for R5 macrophage tropism. (A) Infectivity titers of B33, LN40, and mutant envelopes for HeLa TZM-bl cells that express high levels of CD4 and CCR5 and for RC49 cells that express low levels of CD4. (B) RC49 infectivity evaluated as ratios with TZM-bl cell infectivity and then assessed as a percentage of the ratio for the B33 wt.

HeLa RC49 cells expressing low amounts of CD4 (23) that was more than 100-fold greater than that of LN40 wild type (wt). LN40I conferred only a slight increase in RC49 infectivity compared to that of the LN40 wt. In contrast, the B33T and B33I mutants infected RC49 cells efficiently and within 10-fold of the infectivity for the B33 wt. Thus, the introduction of N283 into LN40 confers substantial infectivity for cells expressing low levels of CD4. However, the reverse substitution, N283T, in the B33 mutant had only a small effect. Isoleucine at residue 283 had the same effect as threonine, conferring only minor effects on B33 and LN40 mutant infectivity of RC49 cells. Similar conclusions were reached when the RC49 infectivity titers for LN40 and each of the mutants were normalized and plotted as a ratio of the infectivity observed for the B33 mutant (see Materials and Methods) (Fig. 1B). These results confirm that an asparagine at residue 283 can have a profound effect on the capacity of HIV-1 R5 envelopes to infect cells via low CD4 levels. However, our data also show that the B33 envelope must carry additional envelope determinants (independent of N283) that confer infection of cells via low levels of CD4.

Chimeric envelope constructs used to map envelope determinants of low CD4 use. To map B33 envelope determinants for low CD4 use, we prepared chimeric envelopes with sequences from B33 and LN40 (Fig. 2). An alignment of the gp120 sequences, including those of B33, B13, B42, LN40, and LN85 from patient NA420, is shown in Fig. 2A. Chimeric envelopes were constructed by using StuI and Bsu36I restriction enzyme sites that are, respectively, situated just downstream from the V2 loop and immediately upstream from the conserved GDPE site in the CD4 binding loop (Fig. 2A and B). To construct the chimeras, we exploited an LN40 envelope construct that carried the gp41 sequences of B33 and which we had shown previously required high levels of CD4 for infection and which infected primary macrophages inefficiently. From results with this construct, it was already clear that LN40 determinants that conferred a requirement for high CD4 levels were located in gp120. In addition, all chimeras were prepared with a threonine residue at 283, since the presence of N283

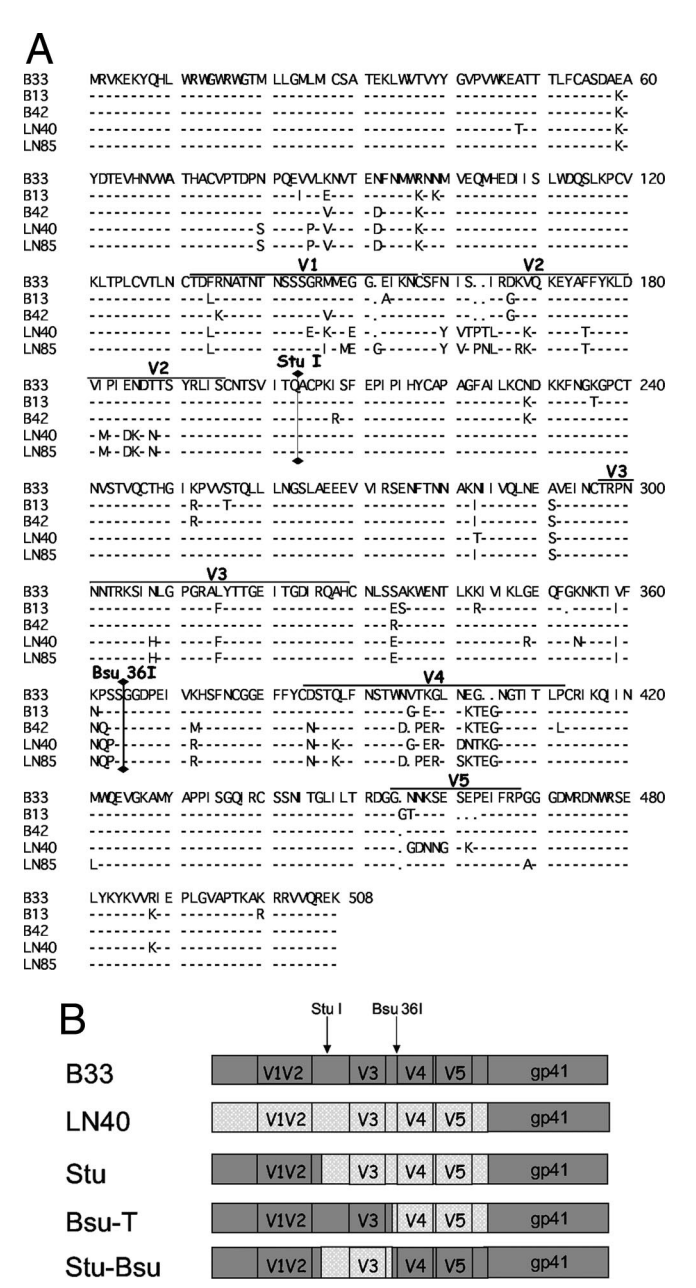


FIG. 2. (A) gp160 amino acid sequence alignment for NA420 env. StuI and Bsu36I restriction sites (vertical lines) used to prepare chimeric envelopes occur after residues Q203 and S364, respectively. Horizontal lines indicate the variable loops. Note that the residue numbering for envelopes in this figure does not precisely follow HXBc2 numbering, which is used throughout the text. Thus, LN40 residues H308, F315, R349, N354, I359, N361, Q362, P363, R372, and N385 are described in the text using HXBc2 numbering as follows: H308, F317, R350, N355, I360, N362, Q363, P364, R373, and N386, respectively. (B) Chimeric B33/LN40 envelopes constructed for mapping determinants of macrophage tropism.

alone substantially increased the capacity of LN40 to use low levels of CD4 for RC49 infection (Fig. 1).

Pseudovirions carrying chimeric envelopes were tested for infection of HeLa TZM-bl and RC49 cells. All the chimeric envelopes conferred high levels of infectivity for HeLa TZM-bl

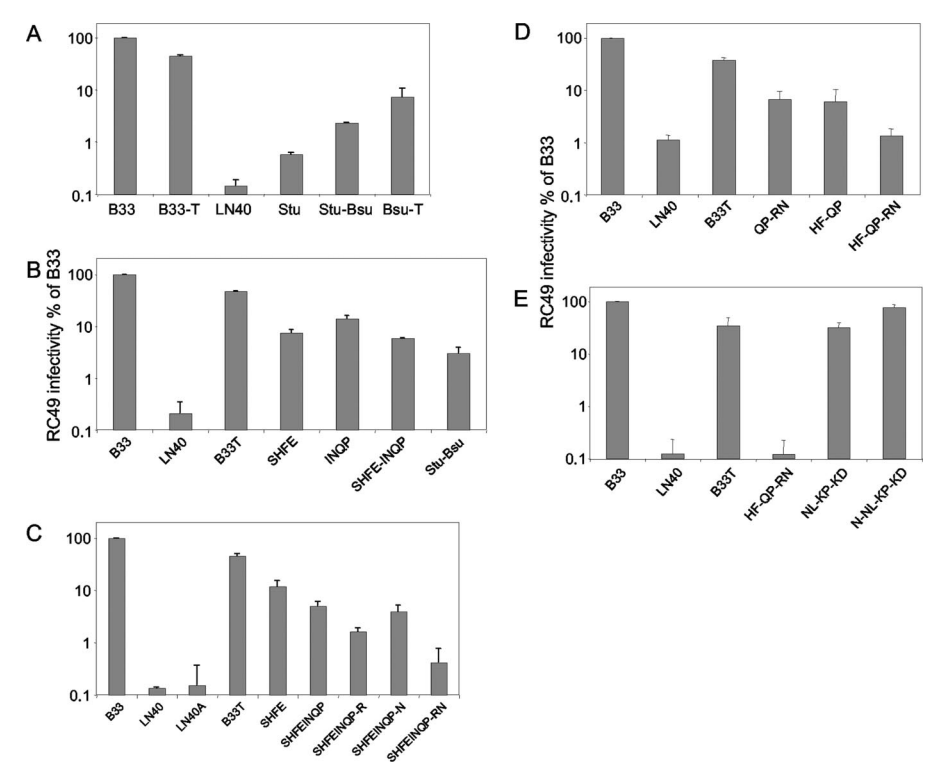


FIG. 3. Identification of gp120 regions responsible for infection of RC49 cells via low CD4. (A) Chimeric env constructs made from B33 and LN40 env. (B) B33, LN40, and mutant B33 env carrying SHFE, INQP, and SHFE-INQP substitutions. (C) B33, LN40, and mutant B33 env carrying R373 and N386 substitutions in combination with SHFE-INQP substitutions. (D) The effect of residues on the N-terminal flank of the CD4 binding loop in combination with downstream residues and determinants in the V3 loop on RC49 infection. (E) B33, LN40, and minimal B33 and LN40 mutants carrying the minimal number of substitutions associated with infectivity for RC49 cells. RC49 infectivity is presented as ratios, with TZM-bl cell infectivity assessed as a percentage of the ratio for B33 (see Materials and Methods). All chimeric and mutant envelopes carried T283 (with the exception of the LN40 N-NL-KP-KD mutant) to eliminate the effects of N283 on RC49 infection.

cells (not shown). The Stu chimera contains LN40 gp120 but carries a segment of B33 gp120, which includes the V1V2 loops. This chimera conferred only a modest increase in RC49 infectivity compared to LN40 (Fig. 3A), indicating that the V1V2 loops do not play a major role in determining infection via low CD4. The Bsu-T chimera infection of RC49 was modestly reduced compared to that by the B33T mutant, implicating an env region stretching from the CD4 binding loop to the gp120 C terminus for infection via low CD4. However, the Stu-Bsu chimera showed a more substantial reduction in RC49 infection, this time implicating a region which includes the V3 loop and the N-terminal flank of the CD4 binding loop.

In summary, two regions of gp120 (from LN40) reduced B33 infection of RC49 cells via low CD4 levels. A region that included the V3 loop and the N-terminal flank of the CD4 binding loop conferred the largest reduction in infection of RC49. However, a smaller reduction in RC49 infectivity was conferred by a gp120 region that included a conserved GDPE motif of the CD4 binding loop and C-terminal sequences up to the junction with gp41.

The role of the Stu-Bsu fragment in RC49 infection via low CD4 levels. We next investigated in more detail the role of the Stu-Bsu region in the infection of RC49 cells via low CD4 levels. This region includes the V3 loop and the N-terminal flank of the CD4 binding loop and contains 11 amino acid differences between B33 and LN40, including the N283T

change for LN40 in the C2 CD4 binding site (Fig. 2A). It should be noted that the numbering system for envelope residues used throughout the text is based on that of HXBc2 and is not precisely the same as shown in Fig. 2A for envelopes from patient NA420 (see Fig. 2 legend).

Since all the chimeras and mutants described carry T283 (unless specifically stated), this residue is not involved in the differences in RC49 infectivity described below. Of the other 10 residues in this region that were different between B33 and LN40, we were tentatively able to rule out the G350R and K355N substitutions in LN40, since LN85 (a second non-macrophage-tropic envelope from patient NA420) carried the corresponding B33 residues, R350 and N355, at these positions (Fig. 2A). We therefore constructed B33 envelope mutants that carried four substitutions on the flank of the CD4 binding loop (INQP), four additional upstream substitutions (SHFE), or all eight substitutions together (SHFE-INQP) and tested their capacity to confer infection of RC49 cells. The SHFE substitutions include S291 (which introduces a potential Nlinked glycosylation signal into the LN40), H308, and F317 residues within the V3 loop and E335.

Both the SHFE and the INQP B33 mutants conferred modest reductions in RC49 infection. All eight substitutions (SHF E-INQP) together conferred the largest reduction in RC49 infectivity, to levels close to those conferred by the Stu-Bsu chimeric envelope (Fig. 3B).

We investigated which residues on the N-terminal flank of the CD4 binding loop affected RC49 infection. Of these residues, the P at residue 364 conferred the maximum reduction in RC49 infectivity, while Q363 conferred a more modest reduction (see Fig. S1A and S1B in the supplemental material). Several mutants carrying two substitutions in this region were therefore also tested. Replacement of B33 PS at residues 363 and 364 with QP also resulted in a reduction in infectivity of RC49 cells, confirming a role for these two residues in the infection of cells via low CD4 levels.

We also evaluated the effect of substitutions upstream from the CD4 binding loop flank using the INQP mutants that carried one or two of the upstream substitutions. Results show that F317 in the V3 loop conferred the greatest reduction in infectivity in conjunction with INQP (see Fig. S1C and S1D in the supplemental material). However, the effect of F317 was enhanced when H308 was also present.

Together, these results show that Q362 and P363 on the N-terminal flank of the CD4 binding loop confer a reduction in infection of RC49 cells via low CD4 levels. However, this reduction is increased by two further substitutions in the V3 loop.

The role of the gp120 fragment, from the BsuI site to the start of gp41, including N386, in the infection of RC49 cells via low CD4 levels. The Bsu-T chimera consists of B33 gp120 carrying LN40 sequences from the CD4 binding loop to the end of gp120 and confers a modest reduction in RC49 infectivity compared to that of B33T (Fig. 3A). This chimera carries the LN40 residue R373 and a potential glycosylation signal at N386, which, as we previously reported, conferred resistance to the CD4 binding site (CD4bs) MAb b12 (7). We first tested an LN40 N386A mutant that eliminated the potential glycosylation site at this position. This mutant showed no increase in RC49 infectivity compared to the LN40 wt, indicating that the glycan at N386 does not have a major impact on tropism on its own. We next evaluated whether the presence of R373 and/or the potential glycosylation site at N386 acted in combination with the upstream SHFE-INQP substitutions to reduce B33 infection of RC49 cells via low CD4 levels. Figure 3C shows that residue R373 or N386 conferred only minimal shifts in RC49 infection when combined with the SHFE-INQP substitutions. However, when R373 and N386 were both combined with the SHFE-INQP substitutions, a more substantial reduction in RC49 infection was observed, with infectivity levels close to those of the background and LN40 infectivity (Fig. 3C). These results suggest that residues R373 and N386 combine with residues on the N-terminal flank of the CD4 binding loop to impact the capacity to exploit low CD4 for infection. We sought to confirm this conclusion by constructing and evaluating B33 mutants that carried only the critical substitutions identified above. Thus, we prepared the B33 HF-QP and QP-RN mutants together with the B33 HF-QP-RN mutant that contains all six residues identified as those involved in RC49 infectivity. Figure 3D shows that the HF-QP and QP-RN mutants conferred a modest reduction in RC49 infectivity compared to those of B33 or B33T. However, when all six substitutions were combined in the HF-OP-RN mutant, only background RC49 infectivity was observed at levels similar to that of LN40. These results confirm that these six residues act

together to confer the loss of RC49 infectivity observed for I N40

Minimal B33 and LN40 mutants with switched tropism phe**notypes.** The data presented above have suggested that a series of residues in the V3 loop and on either side of the CD4 binding loop are those critical for the tropism differences observed for the B33 and LN40 mutants. We next prepared LN40 mutants carrying the minimal number of reciprocal substitutions associated with the capacity to infect RC49 cells via low CD4 levels. The first mutant was constructed with a threonine at residue 283 to avoid the effects of N283 on tropism. Thus, we prepared an LN40 (NL-PS-KD) mutant carrying H308N, F317L (V3 loop substitutions), Q363P, P364S (N-terminal flank of the CD4 binding loop), R373K (C-terminal flank of the CD4 binding loop), and N386D (start of the V4 loop). This NL-PS-KD mutant infected RC49 cells at levels similar to that of B33T, while an additional NL-PS-KD LN40 mutant that also carried N283 conferred levels of RC49 infectivity that were similar to that observed for the B33 wt (Fig. 3E). In comparison, LN40 and B33 HF-QP-RN mutants conferred low or background levels of RC49 infection. These observations strongly indicate that the six residues identified act together to modulate the capacity of B33 and LN40 to exploit low levels of CD4 for infection.

The ability to exploit low CD4 levels on RC49 cells correlates with macrophage tropism. All the data presented so far were derived from experiments that evaluated the infectivity of different envelope mutants and chimeras on RC49 cells, a clone of the HeLa cell line that expresses low amounts of CD4 (23). We next tested a panel of the chimeric and mutant envelopes for their capacities to confer infection of primary macrophages to confirm that infectivity for RC49 cells is a reliable indicator for macrophage tropism (Fig. 4). We tested the infectivity of three different batches of macrophages from different donors. Data from the macrophage batch that showed highest sensitivity to B33 are presented. The infectivity data for other macrophage batches followed the same pattern as that presented in Fig. 4, except for differences in overall titers. In addition, macrophage infectivity data generally followed the same pattern as that recorded for RC49. Thus, B33T conferred a modest reduction in macrophage infectivity compared to that of the B33 wt, while LN40N conferred a 1,000-fold increased infectivity compared to that of the LN40 wt (Fig. 4A). The Stu-Bsu chimera resulted in about a 100-fold decrease in macrophage infectivity compared to the B33T mutant, while infectivity of the Bsu-T mutant was reduced more modestly. Both the SHFE and the INQP mutants showed about a 5- to 10-fold reduction in infectivity for macrophages. However, when these eight substitutions were combined, macrophage infectivity was reduced at least 100-fold, a more substantial reduction than that of the INQP mutant and close to that of LN40 infectivity. This substantial reduction in macrophage infectivity by the SHFE-INOP mutant meant that B33 mutants carrying additional substitutions downstream from the CD4 binding loop, e.g., R373 and N386, further reduced macrophage infectivity only marginally. We subsequently confirmed this observation by testing a B33 T283 HF-QP mutant, which conferred background levels of macrophage infection similar to the LN40 wt (not shown). The minimal B33 (B33 HF-QP-RN) mutant also conferred background macrophage infectivity similar to the

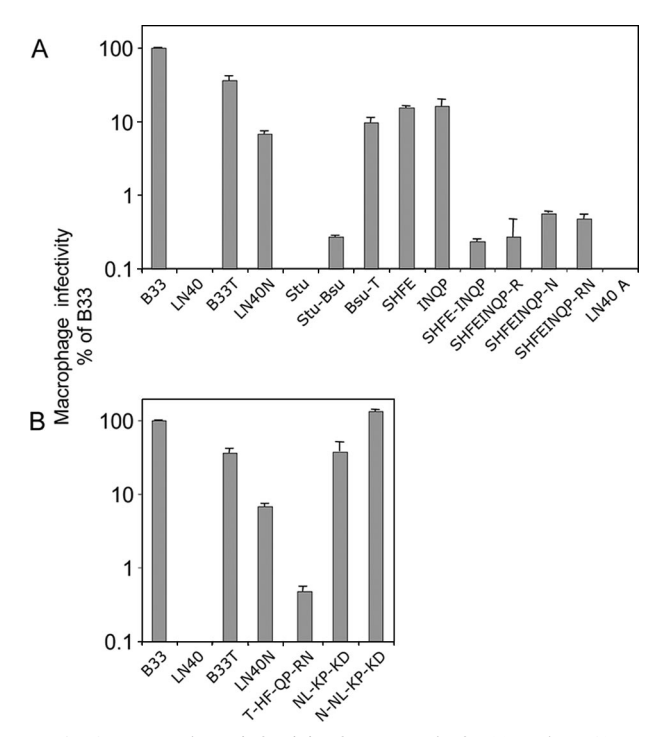


FIG. 4. Macrophage infectivity for a panel of B33 and LN40 mutants. (A) Macrophage infectivity of B33, LN40, and mutant envelopes for primary macrophages. (B) Macrophage infectivity for B33 and LN40 minimal mutants. Infectivity was evaluated as described in Materials and Methods.

LN40 mutant, while (in contrast) the reciprocal LN40 (LN40 NL-PS-KD) minimal mutant conferred substantial infectivity for macrophages (Fig. 4B). Finally, incorporation of N283 into the LN40 minimal mutant further boosted macrophage infectivity to levels similar to that of the B33 wt (Fig. 4B). The infectivity of this panel of B33 and LN40 mutants for macrophages showed a highly significant correlation with infectivity measured with RC49 cells (P < 0.0001).

In summary, our data show that amino acids on the flanks of the CD4 binding loop in combination with residues in the V3 loop are important for macrophage tropism of R5 envelopes. However, residues on the N-terminal flank of the CD4 binding site confer the most significant effects.

Sensitivity to inhibition by PRO 542 (immunoglobulin G-CD4). Recently, we reported that HIV-1 R5 macrophage tropism correlated with sensitivity to sCD4 and to PRO 542, an immunoglobulin G-CD4 construct that is tetrameric for CD4 D1D2 domains (21). Thus, pseudovirions carrying highly macrophage-tropic envelopes were sensitive to inhibition by sCD4 and the more potent PRO 542, while non-macrophage-tropic R5 envelopes were less sensitive or were resistant. These observations are consistent with R5 macrophage tropism being conferred by an increase in env-CD4 affinity. To provide more information about whether B33/LN40 residues, identified as macrophage tropism determinants, may also have an impact on env-CD4 affinity (or act via alternative mechanisms), we tested their effects on the sensitivity to inhibition by PRO 542. Thus, the B33T mutant showed approximately eightfold increased resistance to PRO 542 compared to that of the B33 wt (Fig.

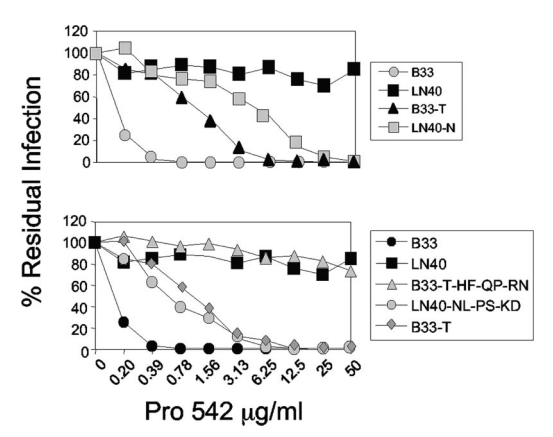


FIG. 5. PRO 542 sensitivity of B33, LN40, and mutants.

5A). In contrast, while the LN40 wt was resistant to PRO 542, the LN40N mutant was sensitive, although it was still more than 30-fold more resistant than B33 wt. These observations reflect the shifts in macrophage and RC49 infectivity observed with the same envelopes and also indicate that additional envelope determinants (over and above residue 283) must modulate PRO 542 sensitivity.

We next investigated the B33 and LN40 mutants, each carrying six reciprocal substitutions that were shown to modulate the infectivity of RC49 cells. Thus, the B33 HF-QP-RN mutant (with T283) was as resistant to PRO 542 as LN40, while the LN40 NL-PS-KD mutant was as sensitive as B33T. These observations indicate that these minimal mutants fully modulated PRO 542 sensitivity and resistance, as well as macrophage tropism (as described above).

We also evaluated the PRO 542 sensitivity of all other B33 and LN40 mutants and chimeras used for mapping the B33/LN40 determinants of macrophage tropism (not shown). PRO 542 sensitivity correlated with the infectivity of RC49 cells (P < 0.0001) and macrophages (P = 0.0005). These results are consistent with macrophage tropism determinants impacting directly on env-CD4 interactions.

DISCUSSION

Here, we have mapped envelope determinants of macrophage tropism by using two R5 envelopes that were amplified directly from patient tissues without culture (20). Patient NA420's B33 was derived from brain tissue and showed high macrophage tropism, while LN40 from lymph node tissue infected macrophages inefficiently. Macrophage infectivity was previously shown to correlate with the capacity to infect cells via low levels of CD4 (20), while Dunfee et al. reported that an asparagine at residue 283 in the C2 part of the CD4 binding site conferred a higher affinity for gp120-CD4 binding (8). Nevertheless, our previous studies implicated additional unknown determinants (20, 22), which we sought to identify in the study reported here. Thus, determinants on the flanks of the CD4 binding loop and on the V3 loop were determined to modulate macrophage infection.

The CD4 binding loop is thought to be the most exposed and perhaps the first part of the CD4bs contacted by CD4 during HIV entry (4). The substitutions identified on the flanks of the

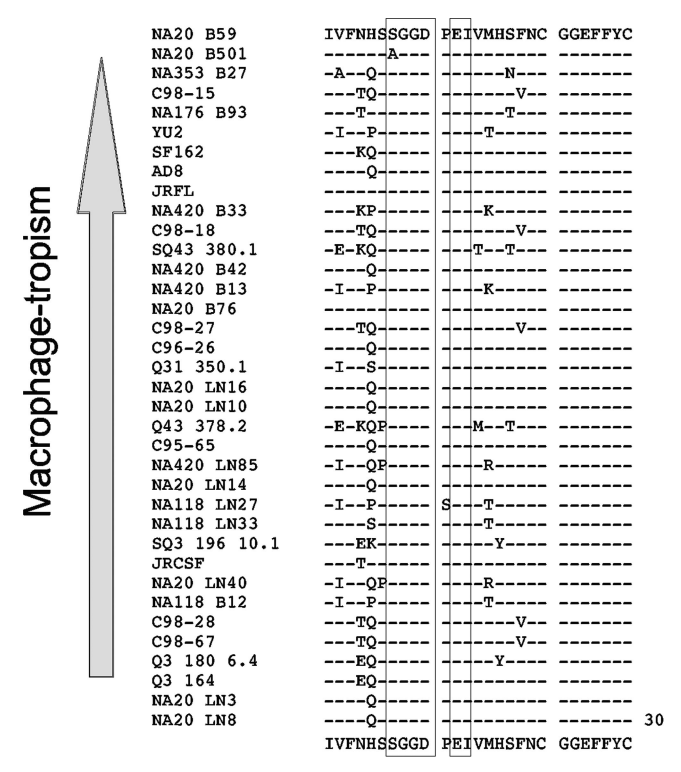
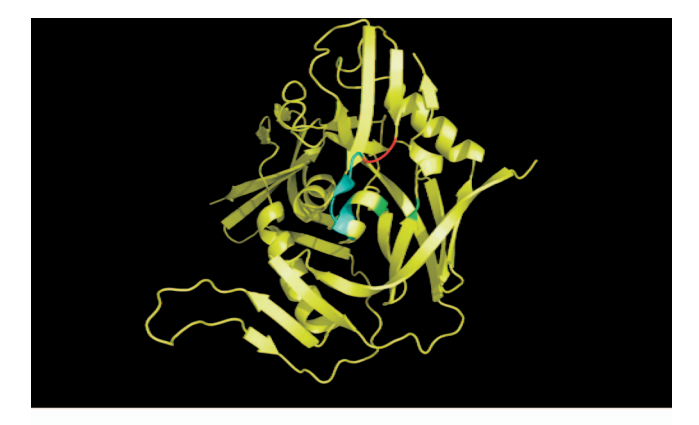


FIG. 6. The N-terminal flank of the CD4 binding loop is variable. A sequence alignment of HIV-1 R5 envelopes previously evaluated for macrophage infectivity (21) is shown.

CD4 binding loop are either directly adjacent to CD4 contact residues or in close proximity (Fig. 6 and 7). We predict that these residues alter the exposure of CD4 contact residues on this loop, thus allowing better access to CD4 and a corresponding increase in affinity for B33. The affinity of the trimeric envelopes for CD4 is not straightforward to evaluate (5). Here, we evaluated the sensitivity of infection to PRO 542, a tetrameric soluble CD4 construct based on immunoglobulin G. An increased affinity of the envelope for CD4 would be expected to result in increased sensitivity to PRO 542, although it is possible that PRO 542 inhibition may be conferred by additional mechanisms. Nevertheless, the B33T and LN40N mutants showed strong shifts in PRO 542 sensitivity toward resistance and sensitivity, respectively (compared to their wt counterparts), as expected for envelopes with altered CD4 binding affinities for gp120 subunits on the trimer. Overall, the capacity of B33, LN40, and a panel of mutants to infect macrophages or RC49 cells via low CD4 levels showed a highly significant correlation with sensitivity to PRO 542, consistent with modulation of env-CD4 affinity.

The N-terminal flank of the CD4 binding loop is variable (Fig. 6), and such residues have been shown to influence gp120-CD4 affinity (15). These flanking residues are adjacent to the highly conserved SGGD-E CD4 contact residues on the apex of the CD4 binding loop. Such variation is consistent with a major impact on the exposure of these CD4 contact residues for this region and is suggestive of an immunity-mediated modulation. Recently, Sterjovski et al. reported that a potential glycosylation site (N362) in this flanking region conferred an



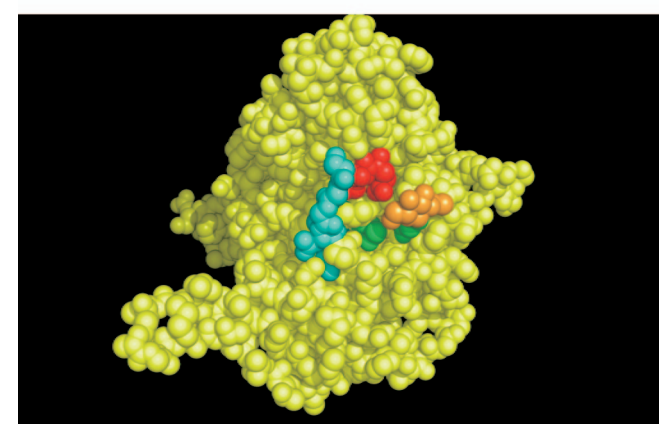


FIG. 7. In the top panel, the proximity of macrophage tropism-determining residues flanking the CD4 binding loop to CD4 contact residues is shown. Residues Q363 and P364 (red) on the N-terminal flank of the CD4 binding loop are adjacent to CD4 contact residues (turquoise) on the apex of the loop. Residues R373 and N386 downstream from the CD4 binding loop are shown in green. In the bottom panel, the glycan at N386 is shown in orange. The structures shown are those of gp120 complexed with CD4 and MAb 17b (15).

increased envelope fusigenicity (25). This observation seems counterintuitive since the presence of a glycan might be expected to shield the CD4 binding loop and reduce the efficiency of gp120-CD4 interactions. Nonetheless, Sterjovski's observations highlight the effect of this region on envelopeinduced fusion. Our results also implicated residues in the V3 loop (H308 and F317 in non-macrophage-tropic LN40) as determinants of R5 macrophage tropism. How these V3 loop residues impact macrophage tropism is less clear, and it is possible that they influence a post-CD4 binding event during entry, e.g., binding to CCR5. However, B33 mutants carrying these residues were less sensitive to PRO 542, consistent with a change in env-CD4 affinity (not shown). The V3 loop extends 30 Å from the gp120-CD4 complex (13). However, the position of the V3 loop on the unliganded envelope is not known, and it is possible that it lies close enough to the CD4 binding loop to influence its exposure. Lynch et al. also reported that a single amino acid change in the V3 loop of a clade C envelope conferred sensitivity to soluble CD4 inhibition (17), consistent with a close association between V3 and the CD4bs.

Our approach in this study was to utilize HeLa RC49 cells as a surrogate for primary macrophages. RC49 cells express low

levels of CD4 (like macrophages) and their use avoids the variation in sensitivity to HIV infection observed for macrophages from different donors. Once the envelope determinants that modulated infection of RC49 cells via low CD4 levels were identified, we tested a representative panel of envelopes, including B33, LN40, and critical mutants, with primary macrophages from several donors. The infectivity data for this panel of envelopes were similar for primary macrophages and RC49 cells. However, the V3 loop (HF) and CD4 binding loop Nterminal flank (QP) residues were sufficient to abrogate macrophage infectivity for B33, without a contribution from downstream residues (R373 and N386) which were required to maximally reduce infectivity for RC49 cells. The mechanistic basis for this difference between macrophage and RC49 infection is unclear but presumably relates to subtly different expression levels of CD4 and/or CCR5 in different cell surface environments. Nonetheless, the levels of infectivity for primary macrophages correlated tightly with those for RC49 cells (P =0.0001). Finally, infectivity titers determined with different macrophage batches varied (reflecting donor variation in sensitivity to infection), although the overall pattern of infectivities remained the same, with B33 as the most macrophagetropic and LN40 as the least.

Our data also provide further information on the role of N283 in macrophage tropism. A T283N substitution in LN40 conferred substantial levels of macrophage infection. The presence of asparagine at residue N283 thus overrules the involvement of additional residues identified here (in the V3 loop and on the flanks of the CD4 binding loop) in macrophage tropism. This could be due to the direct effect of N283 on g120-CD4 binding via the introduction (or improved stabilization) of a hydrogen bond between N283 and Q40 on CD4, as suggested by Dunfee et al. (8). The role of the additional residues identified here presumably involves the modulation of exposure of the CD4 binding loop (as discussed above) affecting env-CD4 affinity without directly altering the CD4 contact residues. Thus, our results indicate that env-CD4 affinity may be modulated by two distinct mechanisms that involve either a direct effect on the CD4bs or an indirect effect that may affect its exposure.

Recently, we reported the determinants in B33 and LN40 envelopes that affect their different sensitivities to the CD4bs MAb b12 (7). B33 is sensitive to b12, while LN40 is resistant. In that study, we showed that the LN40 residues Q363 and P364 on the flank of the CD4 binding loop in combination with the V3 loop residues H308 and F317 conferred a partial shift toward resistance to b12 for B33. However, complete B33 resistance was conferred by a combination of R373 and the glycan at N386. The side chain of R373 and the N386 glycan appear to combine to fill a proximal cavity on gp120 that is targeted by the organic ring on the side chain of W100 on b12 (7). Thus, determinants for macrophage tropism and b12 resistance overlap, although different residues have distinct effects on each phenotype. Our data are consistent with immune modulation of the identified residues during selection of the LN40 envelope in the immune environment of the lymph node. Presumably, the selective force is neutralizing antibodies. In contrast, in brain tissue, where antibodies are usually restricted by the blood brain barrier, envelopes like B33 with a more exposed CD4 binding loop may evolve with an increased sensitivity to neutralization by CD4bs antibodies and an enhanced capacity to infect macrophages via low levels of CD4. Unfortunately, plasma from subject NA420 is not available to test directly whether LN40 is more resistant to neutralization than B33.

In summary, we have identified envelope determinants that modulate R5 macrophage tropism and that have evolved naturally in vivo. The determinants are located on the flanks of the CD4 binding loop but also involve residues in the V3 loop. We predict that they modulate exposure of the CD4 binding loop and accessibility of the CD4bs to CD4. Furthermore, the N-terminal flank of the CD4 binding loop is variable and such variation may contribute to a general mechanism for protecting CD4 contact residues on this loop from neutralizing antibodies. Our data have strong relevance for the design of envelope antigens, which will need to optimally present and expose residues involved in CD4 binding for the induction of neutralizing antibodies targeting this critical and conserved site.

ACKNOWLEDGMENTS

This study was supported by NIH grants AI062514, MH064408, and HD049273.

We acknowledge the University of Massachusetts Center for AIDS Research (CFAR), the AIDS Research and Reference Reagent Program, and the Centre for AIDS Reagents, NIBSC, United Kingdom, for services and reagents.

REFERENCES

- Bleul, C. C., L. Wu, J. A. Hoxie, T. A. Springer, and C. R. Mackay. 1997. The HIV coreceptors CXCR4 and CCR5 are differentially expressed and regulated on human T lymphocytes. Proc. Natl. Acad. Sci. USA 94:1925–1930.
- Brenchley, J. M., T. W. Schacker, L. E. Ruff, D. A. Price, J. H. Taylor, G. J. Beilman, P. L. Nguyen, A. Khoruts, M. Larson, A. T. Haase, and D. C. Douek. 2004. CD4+ T cell depletion during all stages of HIV disease occurs predominantly in the gastrointestinal tract. J. Exp. Med. 200:749–759.
- Carrington, M., M. Dean, M. P. Martin, and S. J. O'Brien. 1999. Genetics of HIV-1 infection: chemokine receptor CCR5 polymorphism and its consequences. Hum. Mol. Genet. 8:1939–1945.
- Chen, B., E. M. Vogan, H. Gong, J. J. Skehel, D. C. Wiley, and S. C. Harrison. 2005. Structure of an unliganded simian immunodeficiency virus gp120 core. Nature 433:834–841.
- Crooks, E. T., P. Jiang, M. Franti, S. Wong, M. B. Zwick, J. A. Hoxie, J. E. Robinson, P. L. Moore, and J. M. Binley. 2008. Relationship of HIV-1 and SIV envelope glycoprotein trimer occupation and neutralization. Virology 377:364-378
- DuBridge, R. B., P. Tang, H. C. Hsia, P. M. Leong, J. H. Miller, and M. P. Calos. 1987. Analysis of mutation in human cells by using an Epstein-Barr virus shuttle system. Mol. Cell. Biol. 7:379–387.
- Duenas-Decamp, M. J., P. Peters, D. Burton, and P. R. Clapham. 2008. Natural resistance of human immunodeficiency virus type 1 to the CD4bs antibody b12 conferred by a glycan and an arginine residue close to the CD4 binding loop. J. Virol. 82:5807–5814.
- Dunfee, R. L., E. R. Thomas, P. R. Gorry, J. Wang, J. Taylor, K. Kunstman, S. M. Wolinsky, and D. Gabuzda. 2006. The HIV Env variant N283 enhances macrophage tropism and is associated with brain infection and dementia. Proc. Natl. Acad. Sci. USA 103:15160–15165.
- Dunfee, R. L., E. R. Thomas, J. Wang, K. Kunstman, S. M. Wolinsky, and D. Gabuzda. 2007. Loss of the N-linked glycosylation site at position 386 in the HIV envelope V4 region enhances macrophage tropism and is associated with dementia. Virology 67:222–234.
- Gao, F., S. G. Morrison, D. L. Robertson, C. L. Thornton, S. Craig, G. Karlsson, J. Sodroski, M. Morgado, B. Galvao-Castro, H. von Briesen et al. for the WHO and NIAID Networks for HIV Isolation and Characterization.
 1996. Molecular cloning and analysis of functional envelope genes from human immunodeficiency virus type 1 sequence subtypes A through G. J. Virol. 70:1651–1667.
- 11. Gorry, P. R., G. Bristol, J. A. Zack, K. Ritola, R. Swanstrom, C. J. Birch, J. E. Bell, N. Bannert, K. Crawford, H. Wang, D. Schols, E. De Clercq, K. Kunstman, S. M. Wolinsky, and D. Gabuzda. 2001. Macrophage tropism of human immunodeficiency virus type 1 isolates from brain and lymphoid tissues predicts neurotropism independent of coreceptor specificity. J. Virol. 75:10073–10089.

- Gorry, P. R., J. Taylor, G. H. Holm, A. Mehle, T. Morgan, M. Cayabyab, M. Farzan, H. Wang, J. E. Bell, K. Kunstman, J. P. Moore, S. M. Wolinsky, and D. Gabuzda. 2002. Increased CCR5 affinity and reduced CCR5/CD4 dependence of a neurovirulent primary human immunodeficiency virus type 1 isolate. J. Virol. 76:6277–6292.
- Huang, C. C., M. Tang, M. Y. Zhang, S. Majeed, E. Montabana, R. L. Stanfield, D. S. Dimitrov, B. Korber, J. Sodroski, I. A. Wilson, R. Wyatt, and P. D. Kwong. 2005. Structure of a V3-containing HIV-1 gp120 core. Science 310:1025–1028.
- Kalter, D. C., M. Nakamura, J. A. Turpin, L. M. Baca, D. L. Hoover, C. Dieffenbach, P. Ralph, H. E. Gendelman, and M. S. Meltzer. 1991. Enhanced HIV replication in macrophage colony-stimulating factor-treated monocytes. J. Immunol. 146:298–306.
- Kwong, P. D., R. Wyatt, J. Robinson, R. W. Sweet, J. Sodroski, and W. A. Hendrickson. 1998. Structure of an HIV gp120 envelope glycoprotein in complex with the CD4 receptor and a neutralizing human antibody. Nature 393:648–659.
- Lee, B., M. Sharron, L. J. Montaner, D. Weissman, and R. W. Doms. 1999. Quantification of CD4, CCR5, and CXCR4 levels on lymphocyte subsets, dendritic cells, and differentially conditioned monocyte-derived macrophages. Proc. Natl. Acad. Sci. USA 96:5215–5220.
- Lynch, R., R. Rong, W. Honnen, J. Mulenga, S. Allen, J. Blackwell, A. Pinter, S. Gnanakaran, and C. A. Derdeyn. 2008. A single residue in the HIV-1 envelope V3 domain modulates exposure of the CD4 binding site, abstr. 242. 15th Conf. Retroviruses Opportunistic Infect., Boston, MA, 3–6 February 2008.
- Mehandru, S., M. A. Poles, K. Tenner-Racz, A. Horowitz, A. Hurley, C. Hogan, D. Boden, P. Racz, and M. Markowitz. 2004. Primary HIV-1 infection is associated with preferential depletion of CD4+ T lymphocytes from effector sites in the gastrointestinal tract. J. Exp. Med. 200:761–770.
- O'Doherty, U., W. J. Swiggard, and M. H. Malim. 2000. Human immunodeficiency virus type 1 spinoculation enhances infection through virus binding. J. Virol. 74:10074–10080.
- Peters, P. J., J. Bhattacharya, S. Hibbitts, M. T. Dittmar, G. Simmons, J. Bell, P. Simmonds, and P. R. Clapham. 2004. Biological analysis of human immunodeficiency virus type 1 R5 envelopes amplified from brain and lymph

- node tissues of AIDS patients with neuropathology reveals two distinct tropism phenotypes and identifies envelopes in the brain that confer an enhanced tropism and fusigenicity for macrophages. J. Virol. **78**:6915–6926.
- 21. Peters, P. J., M. J. Duenas-Decamp, W. M. Sullivan, R. Brown, C. Ankghuambom, K. Luzuriaga, J. Robinson, D. R. Burton, J. Bell, P. Simmonds, J. Ball, and P. Clapham. 2008. Variation in HIV-1 R5 macrophage-tropism correlates with sensitivity to reagents that block envelope: CD4 interactions but not with sensitivity to other entry inhibitors. Retrovirology 5:5.
- 22. Peters, P. J., W. M. Sullivan, M. J. Duenas-Decamp, J. Bhattacharya, C. Ankghuambom, R. Brown, K. Luzuriaga, J. Bell, P. Simmonds, J. Ball, and P. R. Clapham. 2006. Non-macrophage-tropic human immunodeficiency virus type 1 R5 envelopes predominate in blood, lymph nodes, and semen: implications for transmission and pathogenesis. J. Virol. 80:6324–6332.
- Platt, E. J., K. Wehrly, S. E. Kuhmann, B. Chesebro, and D. Kabat. 1998. Effects of CCR5 and CD4 cell surface concentrations on infections by macrophage tropic isolates of human immunodeficiency virus type 1. J. Virol. 72:7855–7864
- Simmonds, P., P. Balfe, J. F. Peutherer, C. A. Ludlam, J. O. Bishop, and A. J. Brown. 1990. Human immunodeficiency virus-infected individuals contain provirus in small numbers of peripheral mononuclear cells and at low copy numbers. J. Virol. 64:864–872.
- 25. Sterjovski, J., M. J. Churchill, A. Ellett, L. R. Gray, M. J. Roche, R. L. Dunfee, D. F. Purcell, N. Saksena, B. Wang, S. Sonza, S. L. Wesselingh, I. Karlsson, E. M. Fenyo, D. Gabuzda, A. L. Cunningham, and P. R. Gorry. 2007. Asn 362 in gp120 contributes to enhanced fusogenicity by CCR5-restricted HIV-1 envelope glycoprotein variants from patients with AIDS. Retrovirology 4:89.
- Veazey, R. S., M. DeMaria, L. V. Chalifoux, D. E. Shvetz, D. R. Pauley, H. L. Knight, M. Rosenzweig, R. P. Johnson, R. C. Desrosiers, and A. A. Lackner. 1998. Gastrointestinal tract as a major site of CD4+ T cell depletion and viral replication in SIV infection. Science 280:427–431.
- 27. Wei, X., J. M. Decker, H. Liu, Z. Zhang, R. B. Arani, J. M. Kilby, M. S. Saag, X. Wu, G. M. Shaw, and J. C. Kappes. 2002. Emergence of resistant human immunodeficiency virus type 1 in patients receiving fusion inhibitor (T-20) monotherapy. Antimicrob. Agents Chemother. 46:1896–1905.